Identification of host-microbiome interactions in nasal diseases using multiomics integration

Yibo Liang[1,#], Zheming Chen[2,#], Chenting Zhang[1,3,#], Zhili Li[1], Jiarui Liu[1], Wenjuan Sun[2], Jianxin Li[2], Jingtai Zhi[1,*], Guimin Zhang[1,*]

Rhinology 63: 6, 753 - 764, 2025

https://doi.org/10.4193/Rhin24.386

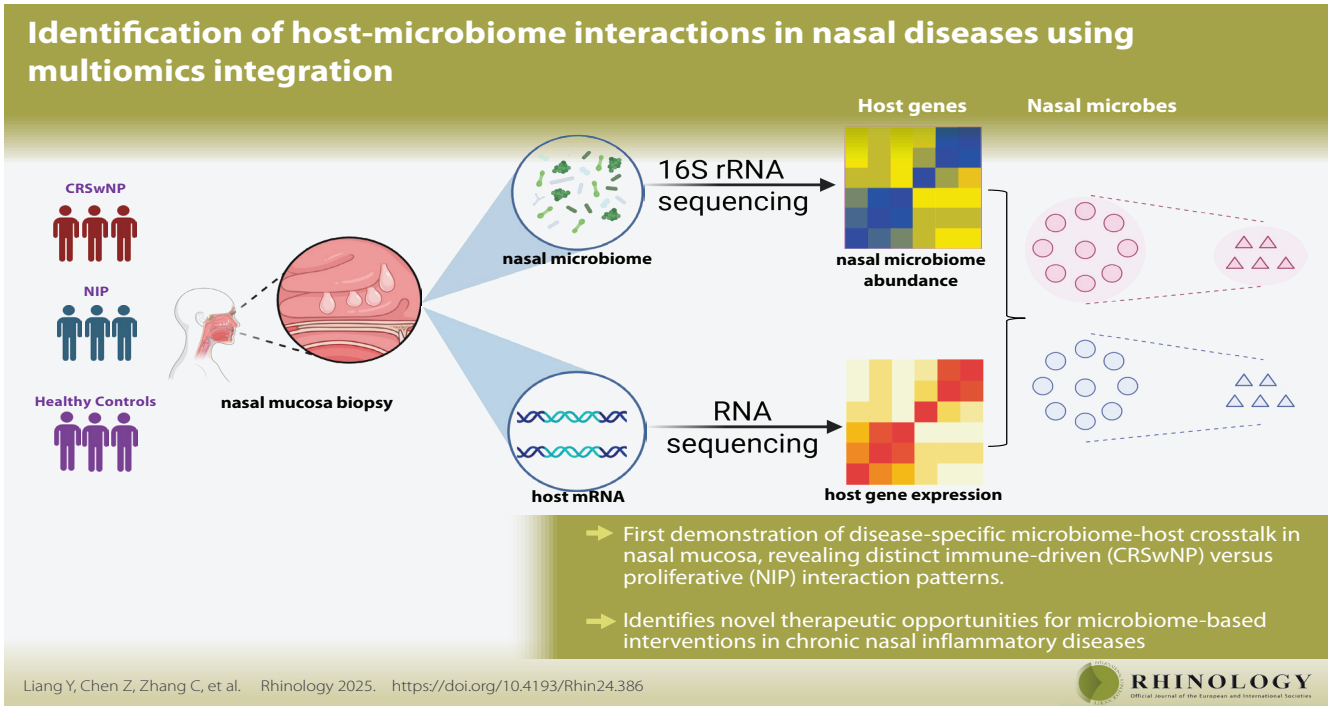

Abstract

Background: Nasal dysbiosis is implicated in the pathogenesis of nasal diseases, yet microbiome-host interplay remains poorly understood.

Methodology: We conducted a cross-sectional analysis comparing 43 CRSwNP patients, 27 NIP patients, and 34 controls using dual 5R 16S rRNA sequencing and host transcriptomics to characterize microbiome profiles and host-microbial interactions.

Results: Distinct microbiome patterns were identified in CRSwNP and NIP mucosal microenvironments. Host-microbiome interaction analysis revealed both shared and disease-specific associations. Common to both disorders were immune-related pathway enrichments, while CRSwNP uniquely demonstrated microbial recognition/immune activation links and NIP showed predominant proliferative pathway correlations. Notably, Bayesian network analysis identified *Geobacillus stearothermophilus* abundance as significantly associated with NF-κB pathway activation in nasal polyps - a finding subsequently experimentally validated.

Conclusion: Our findings delineate disease-specific microbiome-host interplay in nasal pathologies, with CRSwNP exhibiting immune-focused interactions versus NIP's proliferative associations. These insights advance our understanding of nasal disease mechanisms and support the development of targeted microbiome-modulating therapies.

Key words: chronic rhinosinusitis with nasal polyps, nasal inverted papilloma, nasal microbiome, microbiome-host interaction

Introduction

Chronic rhinosinusitis with nasal polyps (CRSwNP) and nasal inverted papilloma (NIP) are two clinically significant nasal diseases characterized by distinct pathophysiology yet shared associations with microbial dysbiosis. CRSwNP, a chronic inflammatory condition, is often linked to immune dysregulation, while NIP, a benign but locally aggressive tumor, carries a risk of malignant transformation [1,2]. Recent studies have implicated specific microbial taxa, such as *Staphylococcus aureus* and human papillomavirus (HPV), in these diseases, but broader microbial-host interactions remain poorly understood [3,4].

Advances in multiomics technologies, including 16S rRNA sequencing and transcriptomics, have provided new opportunities to explore host-microbiome interactions [5]. While these approaches have been applied successfully in other mucosal diseases, such as inflammatory bowel disease and colorectal cancer, similar studies in nasal diseases—particularly those comparing inflammatory and neoplastic conditions like CRSwNP and NIP—are lacking [6,7].

Here, we integrate 5R 16S rRNA sequencing and host transcriptomics to characterize nasal microbial communities and their interactions with host pathways in CRSwNP, NIP, and healthy controls. Using a novel methodological framework combining sparse canonical correlation analysis (sparse CCA) and Bayesian network analysis, we identify distinct microbial signatures and disease-specific host-microbiome interactions. For example, we demonstrate a significant association between *Geobacillus stearothermophilus* and NF-κB pathway activation in CRSwNP, validated experimentally using fluorescence in situ hybridization (FISH) and Western blotting.

This study provides the first comprehensive analysis of host-microbiome interactions in CRSwNP and NIP, offering new insights into their pathophysiology and potential microbiota-based therapeutic strategies. Our methodological framework also lays the groundwork for studying microbial-host interactions in other diseases.

Materials and methods

Subject recruitment and sampling

In this study, a total of 43 patients with bilateral CRSwNP, 27 patients with NIP and 34 controls were recruited. All these subjects underwent surgery, and tissue was retained during surgery for subsequent sequencing analysis. Patients with CRSwNP met the diagnostic criteria of the EPOS2020 guidelines [8]. NIP was determined by postoperative histopathology. The turbinate mucosa tissues of patients with a deviated nasal septum and cranial base operation were included in the control group. The study was approved by the Ethics Committee of Tianjin First Central Hospital. All the subjects were informed in advance and signed informed consent forms.

Exclusion criteria comprised patients with immunological, genetic, hematological (clotting disorders), or cystic fibrosis comorbidities, active sinonasal infections, unilateral nasal polyps, structural sinus abnormalities, or any use of antibiotics, immunosuppressive agents, or corticosteroids (systemic or topical) within the 12-week pre-screening period.

All patients underwent surgical procedures under sterile conditions. Following anesthesia, nasal hair trimming, and disinfection, polyp tissue, tumor tissue, and normal turbinate mucosa were collected under endoscopic guidance. Samples were rinsed with PBS, preserved in RNAlater (Sigma-Aldrich), and immediately refrigerated for downstream analysis. Environmental controls (PBS-only samples) were collected to monitor contamination. Method feasibility and sample quality were validated in preliminary experiments prior to large-scale collection. Detailed protocols are provided in the Supplementary Materials.

Multi-omics sequencing

As previously mentioned, 5R 16S sequencing and RNA-seq data was used in this study [9-11]. Detailed methods are shown in the Supplementary Materials.

5R 16S rRNA gene sequencing and analyses of negative controls

To minimize low-abundance noise, sequences with <1,000 total reads (including negative controls) and taxa with relative abundance $<10^{-4}$ were excluded. Contaminants were identified as genera present in ≥50% of negative controls (≥3 samples at >0.001% abundance) and removed from nasal tissue data, followed by renormalization to obtain true microbial abundances.

Sparse CCA analysis

We applied a machine learning framework [5] to integrate host gene expression and microbiome data using sparse canonical correlation analysis (sCCA). Optimal hyperparameters ($\lambda1 = 0.2$, $\lambda2 = 0.15$ for CRSwNP; $\lambda1 = 0.266$, $\lambda2 = 0.177$ for NIP) were determined via leave-one-out cross-validation. The model identified top 10 components per cohort, retaining only significant associations (FDR < 0.1 after Benjamini-Hochberg correction). CRSwNP yielded 3 key components (mean: 1739 genes, 4.5 microbes), while NIP yielded 6 (mean: 2786 genes, 6.4 microbes). Analyses used R/PMA (v4.2.0/1.2.1) with visualization in Cytoscape (v3.10.0). Detailed methods are described in the Supplementary Materials.

Inference of microbial-host interaction networks

In addition to identifying differential pathways, identifying important directional edges between pathways can also provide valuable insights when studying microbe-host interactions. The path interaction network (Bayesian Network analysis) was used with the "CBNplot" package to construct the gene interaction network [12]. Based on the host expression profile data, associ-

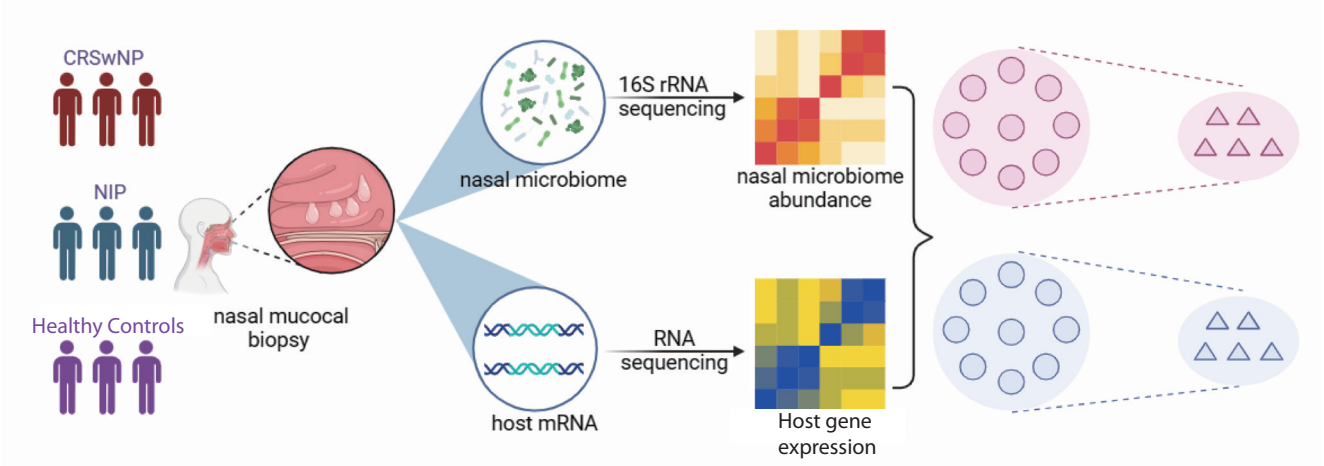

Figure 1. Schematic diagram of the experimental workflow framework. Nasal mucosal tissue was collected from individuals in each disease cohort. Paired host transcriptome data and nasal microbiome abundance data, which were generated for each sample, were integrated using a machine learning-based framework to characterize the association between the nasal microbiome and host genes in the two disease pathways.

ated microorganisms were screened out in combination with sparseCCA, the interaction direction was calculated, the bnpathplot function was used to obtain the interaction direction and intensity, and Cytoscape was used to plot the network.

Fluorescence in situ hybridization (FISH)

According to previous methods [13], the *Geobacillus* FISH probe was hybridized to tissue sections and labeled with FITC at the 5' and 3' ends (5'CCGAATCAAGGCAAGCCCCAATC-3'). This probe was designed and synthesized by Exonbio (Gungzhou, China). This probe targets *Geobacillus stearothermophilus*, and some *Geobacillus* sp. EUB330 proteins target a conserved domain of bacterial 16S rRNA. FISH images were captured with a Nikon 80i microscope. The images were analyzed and scored according to the fluorescence signal.

Western blotting

Tissue samples were homogenized in liquid nitrogen and lysed with RIPA buffer. Following centrifugation, protein concentration was measured using the BCA assay. Proteins were separated by electrophoresis, transferred to membranes, blocked with BSA, and incubated overnight at 4°C with primary antibodies (anti-p65, anti-p-p65, anti-β-actin). After washing, membranes were incubated with secondary antibody for 1 h, with the blots shown in Figure S1.

Results

The nasal microbiomes of CRSwNP and NIP patients are distinct

This study enrolled 43 bilateral CRS patients, 27 NIP patients, and 34 controls (demographics in Table S1). We performed deep 5R 16S rDNA sequencing to characterize tissue-resident microbiota (Figure 1), with rarefaction curves demonstrating sufficient sequencing depth to capture species-level diversity (Figure S2A-B). Alpha diversity analysis revealed significantly reduced microbial diversity in CRSwNP compared to controls (Figure S2C), while NIP and control groups showed comparable diversity (Figure S2D). These findings suggest distinct microbiome profiles associated with CRSwNP pathogenesis, potentially reflecting disease-specific ecological alterations in the nasal mucosal environment.

To assess the overall diversity in the microbial composition, we performed principal coordinate analysis (PCoA) based on the Bray-Curtis dissimilarity for microbiome data at the species levels. There were partial but significant differences in classification characteristics between patients with CRSwNP and controls (R^2=0.019, P<0.001; Figure 2A). Similar findings were observed in NIP patients and controls (R^2=0.047, P=0.045; Figure 2B). In addition, a partial but significant difference in categorical characteristics was observed between patients with CRSwNP and those with NIP (R^2=0.250, P<0.001; Figure S2E). These results suggest that patients with nasal diseases have different microbiome characteristics from those of normal people and that the two diseases have their own unique microbiome characteristics.

This study revealed distinct microbiome profiles across disease groups at multiple taxonomic levels. *Proteobacteria*, *Actinobacteria*, and *Firmicutes* dominated the phylum-level composition of CRSwNP and NIP (Figure S2F-G). Taxonomic analysis identified disease-specific enrichment patterns: *Aquabacterium* predominated in CRSwNP patients while *Corynebacterium* dominated NIP cases, a pattern conserved from genus to species level (Figure 2C-D, Figures S3A-B, 4A-B). LEfSe analysis confirmed these differential abundances (LDA>2, p<0.05), with CRSwNP showing enriched *Aquabacterium*/*Sphingomonas* and depleted *Bacteroides* (Figure S3C), while NIP exhibited increased *Haemophilus*/*Mycobacterium* and decreased *Gardnerella* (Figure S3D).

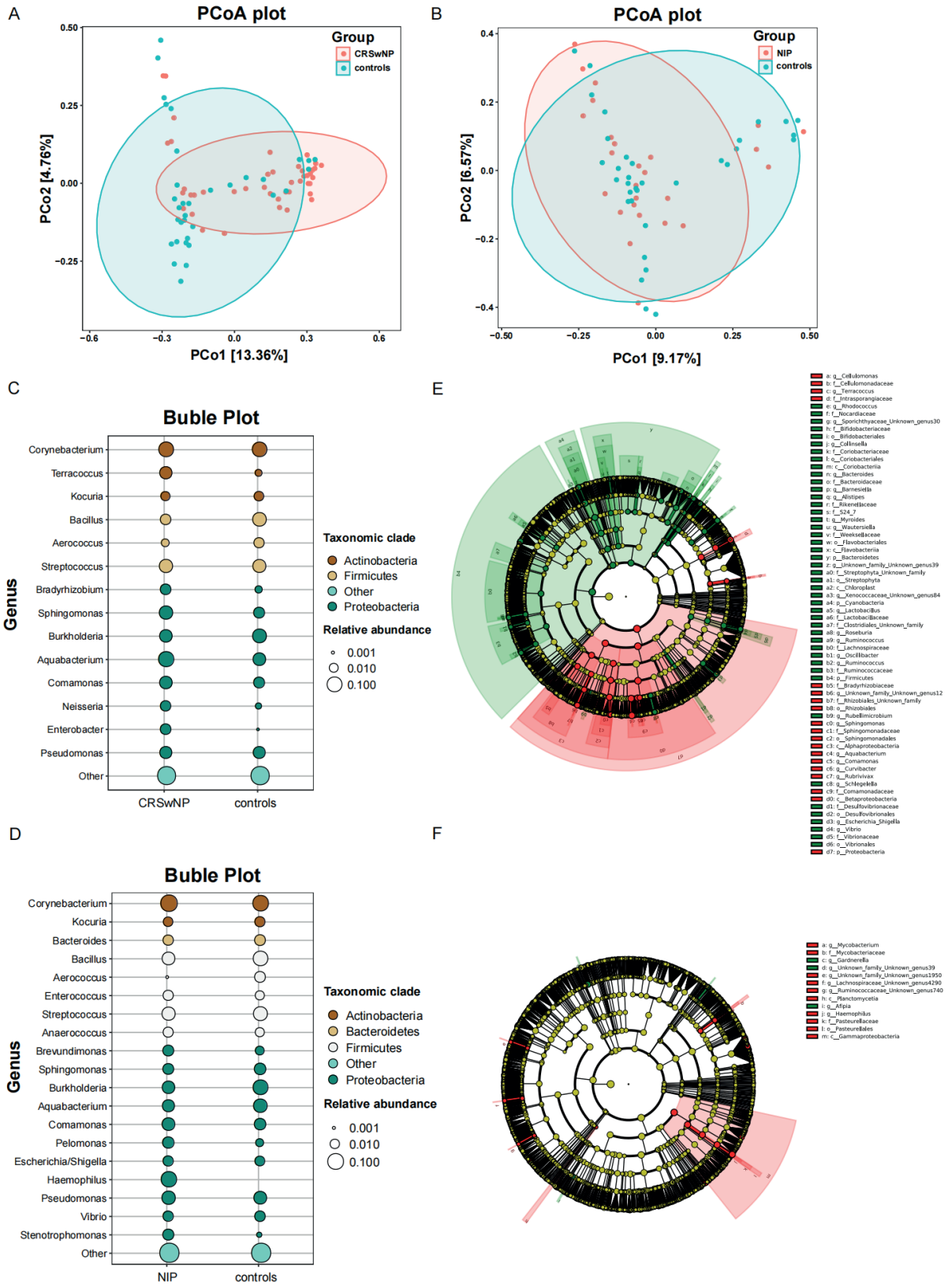

Figure 2. Microbiome analysis of patients with nasal diseases. PCoA indicates a partial but significant separation between patients with CRSwNP (A)/ NIP (B) and controls. Bubble plot of the nasal genus affiliation to phylum with different colors and the abundance of genera with bubble size in patients with CRSwNP (C)/ NIP (D) and controls. Predominant taxa distribution between groups in a phylogenetic tree with cladogram computed by LDA effect size analysis. The circles radiating from inside to outside represented the classification level from Kingdom to Species. Taxa with significant differences are highlighted and labeled between CRSwNP (E)/NIP (F) and the control groups. PCoA, principal co-ordinates analysis.

Host transcriptomes of CRSwNP and NIP patients

The host transcriptomes of 40 CRSwNP samples, 20 NIP samples, and 20 control samples were analyzed. Principal component analysis (PCA) revealed significant differences among the CRSwNP, NIP, and control groups (Figure 3A, Supplementary Figure 4A, B and C). To identify potential target genes that were closely related to CRSwNP and NIP, differential expression analysis of the CRSwNP, NIP and control groups was performed (FDR < 0.01, fold change (FC) > 1.5). A total of 4456 differentially expressed genes were identified between the CRSwNP group and the control group (Figure 3B). KEGG analysis revealed that the top 20 pathways associated with differentially expressed gene enrichment were cytokine–cytokine receptor interaction, neuroactive ligand–receptor interaction and metabolic pathways and pathways in cancer (Figure 3D). There were 6040 differentially expressed genes between the NIP and control groups (Figure 3C). KEGG analysis suggested that the top 20 pathways of differentially expressed gene enrichment included metabolic pathways, pathways in cancer, neuroactive ligand-receptor interactions, cytokine-cytokine receptor interactions and other pathways (Figure 3E). These results suggest that the immune, metabolic and cell proliferation pathways of the CRSwNP and NIP groups are significantly different from those of the control group. Therefore, hierarchical clustering of all differentially expressed genes showed clear separation between all three groups (Figure 3F), confirming distinct transcriptional landscapes.

The disease-specific nasal microbiome is associated with different host pathways

Since different nasal diseases have unique nasal microbiota characteristics, we hypothesized that changes in the CRSwNP and NIP transcriptomes may be partly related to the nasal microbiota and that there may also be microbiota-host interactions involved in nasal diseases. To investigate this possibility, we performed transcriptomic sequencing of the samples at the same time as microbial sequencing. We obtained 80 pairs of paired data related to the nasal microbiome and host gene expression, including 40 pairs in the nasal polyp cohort, 20 pairs in the NIP cohort, and 20 pairs in the control cohort. Follow-up analysis was also conducted.

Previous studies have suggested that microbes that are involved in the same biological function may interact with host genes in the form of groups [5]. Considering the challenges of integrating multiomics data with high dimensionality, sparsity, and multicollinearity, we used sparse CCA to explore nasal microbiome-host interactions. This approach facilitates characterization of the association between host transcriptome expression and nasal microbiome abundance in both nasal diseases at the population level. In this study, sparseCCA was first used to reduce the dimension of the gene expression profile and microbial abundance table to gather potentially related features together and then to identify multiple microbial and host pathways/genes that may be related to reduce the computational burden and interference features of the next analysis and improve the analysis accuracy. SparseCCA is used to define host genes or microorganisms with potentially related features that clustered together as components. By fitting sparse CCA models to the transcriptome and microbiome datasets of each disease cohort, host gene components that were significantly associated with the nasal microbiome were identified. We then performed pathway enrichment analyses of host genes for these components, which were significantly associated with the nasal microbiome, to identify the host pathways that were associated with the nasal microbiome in both nasal diseases.

In this study, we found a population-level association between host transcriptome expression and nasal microbiome abundance in two nasal diseases. In the nasal polyp group, there was a correlation between the host transcriptome and the abundance of the nasal microbiome in three components. In the NIP group, associations between host transcriptome expression and nasal microbiome abundance were identified in six components. Through preliminary gene annotation and pathway analysis, 226 host pathways (FDR < 0.1) were identified in the two nasal diseases, mainly including immune, metabolic, host defense and cell proliferation pathways. Some of these relationships have been confirmed. These results suggest that the host transcription profile of patients with CRSwNP may be partially influenced by the nasal microbiota.

To visualize the host transcription profiles that are affected by nasal microbiota in nasal diseases, we performed GSVA on the enriched pathways in the associated components and identified the top 20 pathways for each component (Figure 4A). We found that nasal microbes mainly affect host metabolism, the immune response, host defense function, and other processes. In addition, we found that the effects of the nasal microbiome on host transcriptional profiles are significantly different in different nasal diseases. Among them, in CRSwNP, the nasal microbiome mainly affects host metabolism-related and immune response-related pathways. For example, Th17 cell differentiation, Th1 and Th2 cell differentiation and the NF-κB signaling pathway have been proven to have important effects on the pathophysiological processes of CRSwNP. In NIP, nasal bacteria affect signal transduction pathways. For example, glycosaminoglycan biosynthesis-keratan sulfate is closely related to the occurrence and development of many tumors. In addition, it affects a variety of amino acid metabolic pathways, such as D-glutamine and D-glutamate metabolism. The nasal microbiome may play a crucial role in the occurrence and development of different nasal diseases.

In addition, previous studies have shown that there are "shared" and "disease-specific" pathways in the intestinal microbiome in

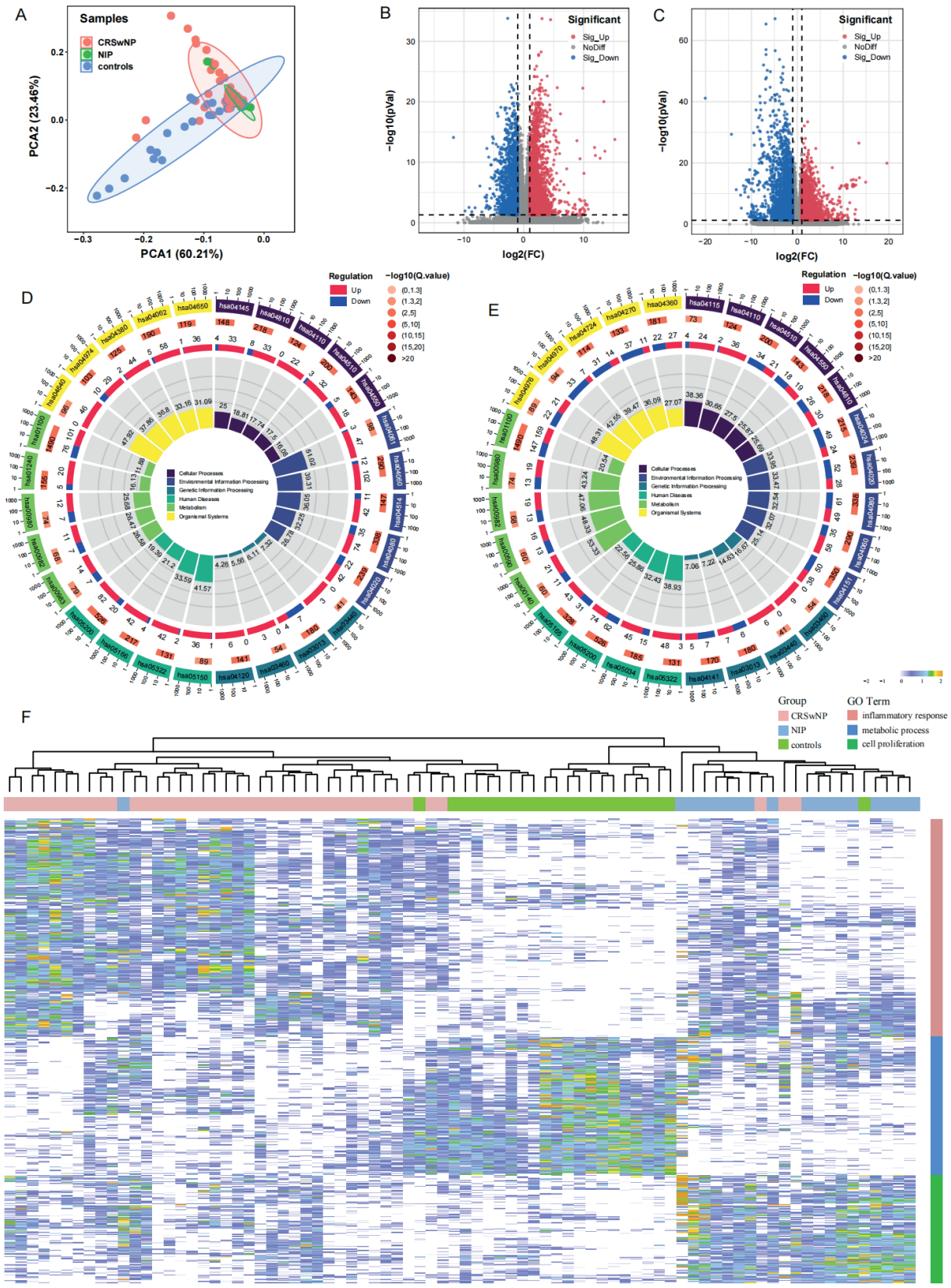

Figure 3. Host transcriptome analysis of patients with nasal diseases. (A) Principal component analysis indicates significant separation among CRSwNP, NIP and controls for host transcriptome. Volcano plot showing differentially expressed genes between the CRSwNP (B)/ NIP (C) and controls. (D) The KEGG LoopCircos showed KEGG pathway enriched with Top comparing CRSwNP and controls. (E) The KEGG LoopCircos showed KEGG pathway enriched with Top comparing NIP and controls. (F) Heatmap of inflammatory response related, metabolic process related and cell proliferation related among CRSwNP.

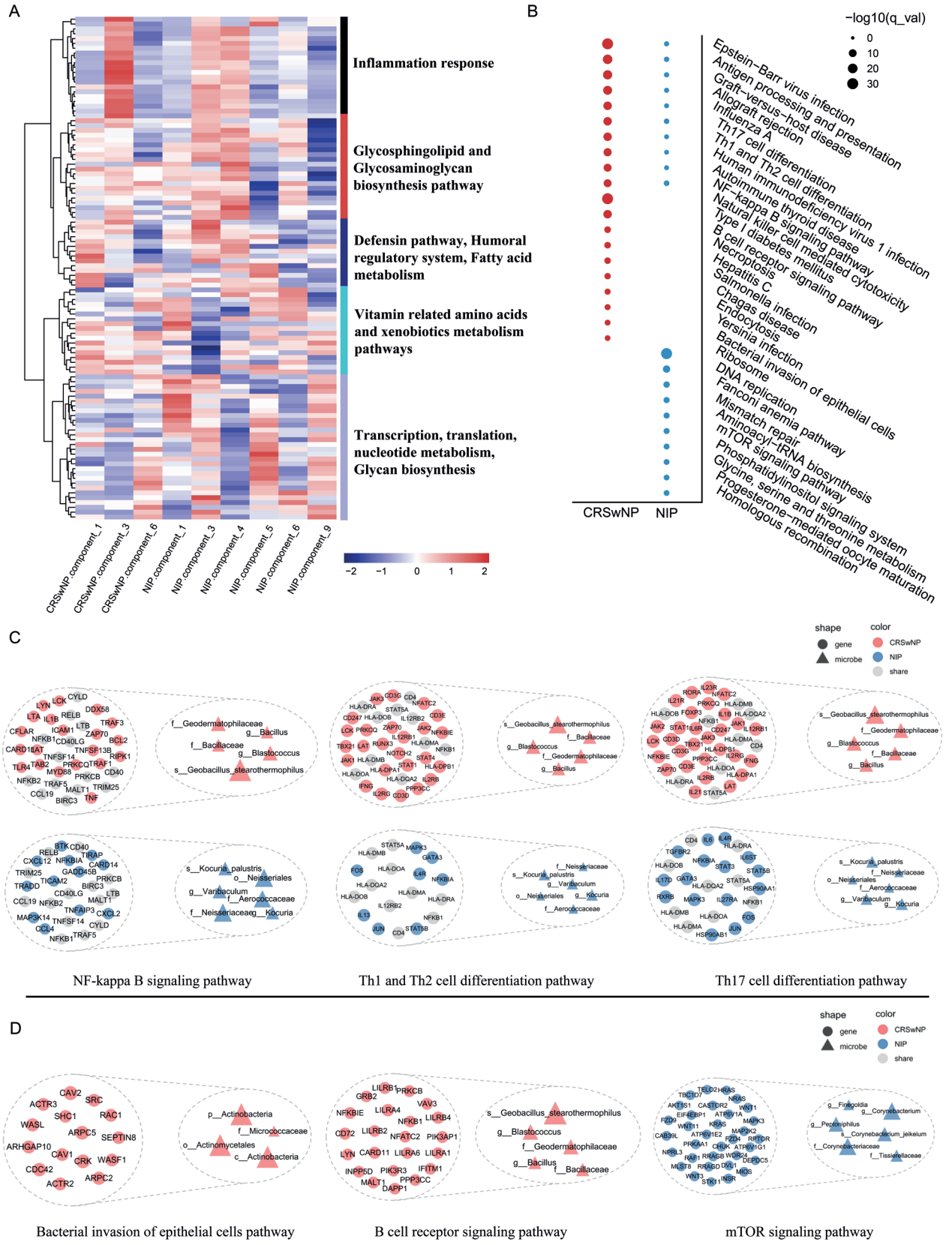

Figure 4. Sparse CCA analysis showed mucosal host–microbe interaction modules in nasal diseases. (A) GSVA analysis presented the top 20 pathways for each component in nasal diseases. (B) Host pathways enriched for sparse CCA gene sets associated with nasal microbiome composition across diseases. (C) Association between microbial taxa in CRSwNP and NIP and host genes in the Th17 cell differentiation, Th1 and Th2 cell differentiation and NF-kappa B signaling pathway. Genes that are common between pathways or components across two disease cohorts are shown in grey. (D) Association between the set of host genes in disease-specific host pathway.

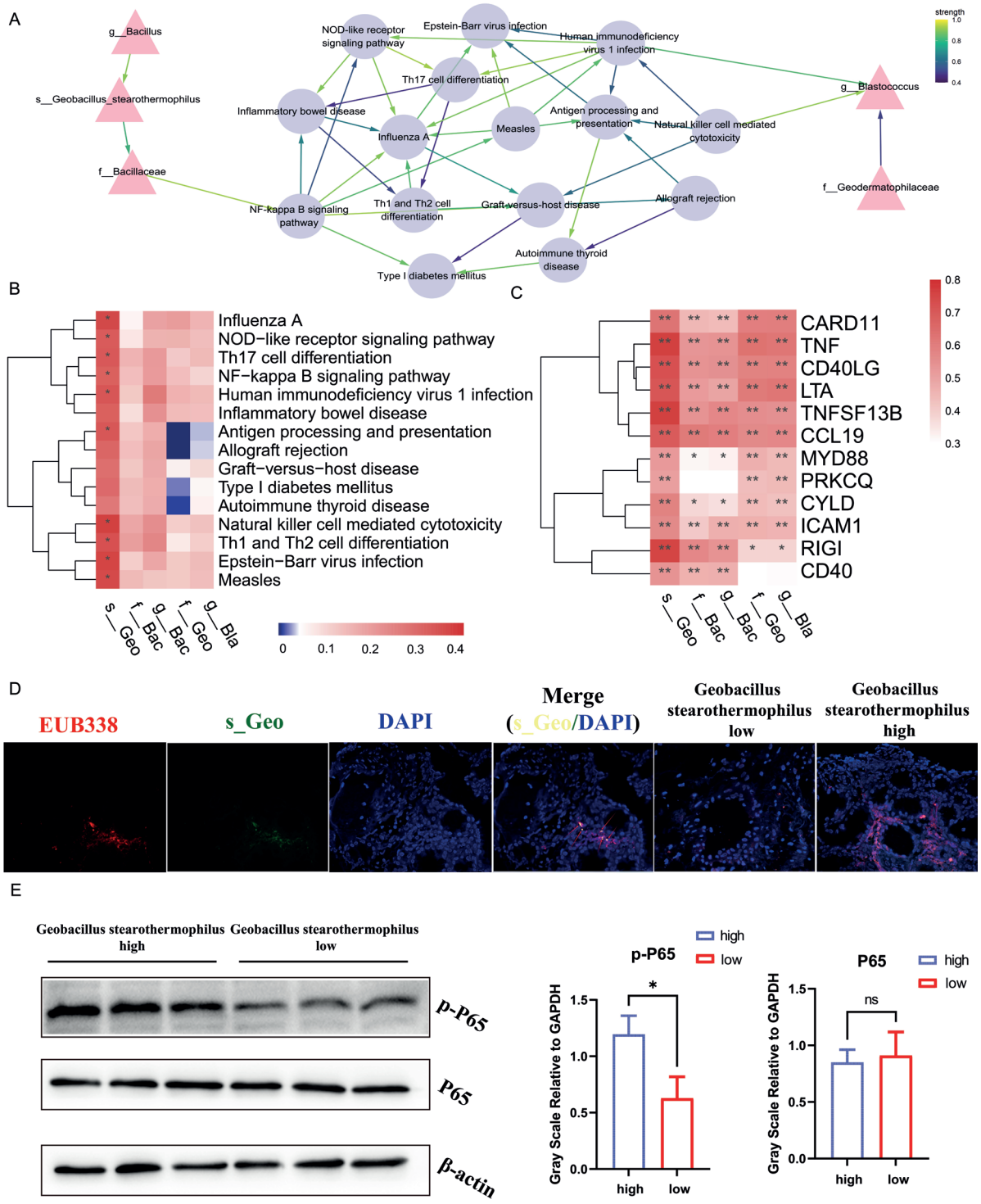

Figure 5. The abundance of *Geobacillus stearothermophilus* in CRSwNP was significantly correlated with NF-κB pathway activation. (A) Based on Bayesian networks, *Geobacillus stearothermophilus* in component 3 of the CRSwNP group could significantly affect the host NF-κB pathway. (B) Heatmap showed association between microbial taxa and host genes in component 3 of the CRSwNP group. (C) Association between microbial taxa and host genes in the NF-κB pathway in component 3 of the CRSwNP group. (D) Representative images of FISH detecting *Geobacillus stearothermophilus* in CRSwNP. FISH using an Cy3-conjugated "universal bacterial" 16S rRNA-directed oligonucleotide probe (EUB338, red); and FITC conjugated *Geobacillus stearothermophilus* 16S rRNA-directed oligonucleotide probe (green) demonstrates the presence of bacteria within the nasal mucosa of CRSwNP samples. Epithelial cell nuclei were stained with DAPI. 200×magnification. (E) Western blot analysis of the NF-κB pathway between high and low abundance *Geobacillus stearothermophilus*. * represents $p<0.05$ and ** represents $p<0.001$. n=40 in CRSwNP patients, n=18 in NIP patients and n=22 in controls. CRSwNP, chronic rhinosinusitis with nasal polyps; NIP, nasal inverted papilloma. f__Bac; f__*Bacillaceae*_1; f__Geo, f__*Geodermatophilaceae*; g__Bac, g__*Bacillus*; g__Bla, g__*Blastococcus*; s__Geo, s__*Geobacillus_stearothermophilus*.

different intestinal diseases. The "shared" pathway is the host pathway that is associated with the microbiome that is present in different diseases. Additionally, "disease-specific" pathways are host pathways that are associated with the microbiome that are present only in a single disease. Therefore, we hypothesized that this "shared" and "disease-specific" pathway also exists in nasal diseases. In our study, we found a total of 89 shared that are pathways associated with the nasal microbiome. For simplicity, we focused on the top ten most important shared and disease-specific pathways (Figure 4B). We found that the shared pathways that are associated with nasal disease in both nasal disease groups were associated with immune response-related pathways. Examples include Th17 cell differentiation, Th1 and Th2 cell differentiation, and the NF-κB signaling pathway (Figure 4C) [14,15]. These pathways are associated with local immune disorders and the promotion of inflammation in sinusitis. In NIP, Th17 cell differentiation and Th1 and Th2 cell differentiation are associated with the breakdown of the epithelial barrier [16]. These results suggest that the nasal microbiome can promote the development of disease by promoting the immune response in patients with different nasal diseases.

In addition, we identified "disease-specific" pathways that are associated with nasal flora, including 24 CRSwNP-specific pathways and 113 NIP-specific pathways. In CRSwNP, the nasal microbiome mainly affects host recognition and the immune response. For example, the B cell receptor signaling pathway plays a crucial role in the effect of various immune cells in CRSwNP, and the nasal microbiome plays a role through the bacterial invasion of epithelial cells pathways (Figure 4D) [17,18]. The nasal microbiome in NIP mainly affects host functions. For example, the mTOR signaling pathway can facilitate this process (Figure 4D) [19]. These results suggest that the nasal microbiome plays a distinct and important role in different nasal diseases and may play a crucial role in the occurrence and development of the disease.

The abundance of *G. stearothermophilus* in CRSwNP is correlated with NF-κB pathway activation

These results suggest that the host transcription profile of nasal diseases may be partially influenced by the nasal microbiota. To provide an initial validation of our findings, based on Bayesian networks, we looked for the strongest possible pair of bacteria-host pathway relationships among the different components. Based on Bayesian networks, we found that *G. stearothermophilus* in component 3 of the CRSwNP group could affect the host NF-kB pathway (Figure 5A). Spearman correlation analysis further revealed that the abundance of *G. stearothermophilus* was positively correlated with the NF-κB pathway, a key driver of inflammation in nasal polyps (all $P<0.05$; Figure 5B and C). To verify this finding, high- and low-abundance specimens of *G. stearothermophilus* were selected for comparison. First, FISH was used to verify the presence of *G. stearothermophilus* in high- to low-abundance samples (Figure 5D). Then, western blotting was used to verify the activation of the NF-κB pathway in the *G. stearothermophilus* tissue samples. WB results showed that high-abundance of *G. stearothermophilus* in CRSwNP is positively correlated with p-P65 expression ($P=0.017$), but the protein expression of P65 was not affected ($P=0.683$; Figure 5E). Our results suggest that the abundance of *G. stearothermophilus* is significantly correlated with NF-κB pathway activation in nasal polyps. Based on a series of analyses, such as sparseCCA and Bayesian network analyses, we screened the effect of *G. stearothermophilus* on the host NF-κB pathway and verified its interaction through immunofluorescence experiments. Our analytical method can be used to screen for more reliable and accurate microbe-host interaction mechanisms from large amounts of microbial and transcriptome data within a limited computational link, improve the analysis efficiency, and provide a new approach for the study of nasal diseases.

Discussion

The nasal cavity harbors complex microbial communities that dynamically interact with the host [20,21]. While previous studies have characterized nasal dysbiosis, the tripartite relationship among microbiota, host responses, and disease mechanisms remains poorly understood [22,23]. Through integrated analysis of mucosal gene expression and microbiome profiles in CRSwNP and NIP patients, we reveal novel host-microbe interactions that may advance the development of microbiota-targeted therapies for nasal inflammatory diseases.

The mucosa serves as a critical host-microbial interface, with emerging evidence linking mucosal dysbiosis to chronic inflammatory and neoplastic diseases [24,25]. Here, we show that distinct nasal disorders exhibit disease-specific microbial signatures. Our findings suggest that nasal mucosal microbiota may actively participate in disease pathogenesis, beyond merely reflecting inflammatory microenvironments.

Previous studies have only described changes in the microbiome of nasal disease patients, and the impact of these changes on the host is unknown. To this end, we further characterized the association between the nasal microbiome and host genes by analyzing both the microbiome and the host transcriptome in nasal tissue. In this regard, through biogenic analysis, we found that nasal microorganisms may affect the host immune, metabolic, defense and cell proliferation pathways. Some of these bacteria-host interaction pairs have been confirmed. For example, *Lactobacillaceae* can improve diabetes-related symptoms by activating the PI3K-Akt signaling pathway in patients with diabetes. Additionally, *Lactobacillus* was found to be closely related to propanoate metabolism in Parkinson's disease patients [26-28]. These results suggest that the host transcription profile of patients with nasal disease may be partially influenced

by the nasal microbiota.

While prior research has examined microbiome-pathology relationships in isolated diseases, our comparative analysis of mucosal-microbial interactions across nasal disorders reveals both shared and disease-specific mechanisms. We demonstrate that nasal microbiota consistently modulates immune pathways (Th1/Th2/Th17 differentiation, NF-κB signaling) in both CRSwNP and NIP, suggesting a common immunostimulatory role in disease progression [14-16]. Notably, we identified disorder-specific patterns: CRSwNP microbiota preferentially activate B-cell receptor signaling [17,18], whereas NIP-associated flora alters host metabolic regulation via mTOR pathways [19]. These findings establish that nasal microbes contribute to disease pathogenesis through both pan-inflammatory mechanisms and disease-tailored functional modules, highlighting new targets for precision interventions.

Geobacillus stearothermophilus, a Gram-positive thermophilic bacterium, may play a role in CRSwNP, though its involvement remains unexplored and merits further investigation. This study has innovatively revealed the key role of *Geobacillus* in the pathogenesis of CRSwNP through the specific activation of the NF-κB signaling pathway. Through integrated analysis of 16S rRNA sequencing and transcriptomics, we found a significant correlation between the enrichment of *Geobacillus* in the nasal cavities of CRSwNP patients and the activation of NF-κB. Western blot and FISH validation experiments showed that the level of p-P65 selectively increased in the nasal mucosa of these patients, while the expression of total P65 remained unchanged, clearly confirming that the microbiota activates the NF-κB pathway through a specific rather than a broad mechanism. This finding has significant clinical implications: as a core regulatory factor of pro-inflammatory responses, the activation of NF-κB can induce the expression of various cytokines, thereby promoting Th2 immune responses and eosinophil recruitment, forming a mechanistic loop with the previously reported association between *Geobacillus* and increased eosinophils [22,29]. Notably, this "microbe-NF-κB axis" suggests that *Geobacillus* may maintain chronic inflammation by activating innate immune sensors (such as Toll-like receptors), leading to sustained NF-κB activation. These results establish the molecular bridge role of NF-κB between nasal microbiota dysbiosis and the characteristic inflammatory environment of CRSwNP, providing a new theoretical basis for the development of targeted therapeutic strategies for the NF pathway.

While our study provides valuable insights into host-microbiome interactions in nasal pathologies, several limitations must be acknowledged. First, reliance on 16S rRNA gene sequencing, rather than metagenomic sequencing, restricts the resolution of taxonomic classification at the species level, potentially limiting data interpretation. Second, although we employed a multi-omics approach to explore microbiome-host relationships, further validation through in vitro and in vivo experiments is necessary to confirm our findings. Finally, since this was a single-center study, future multi-center investigations incorporating diverse geographic populations will be essential to enhance the generalizability of our conclusions. Addressing these limitations in subsequent research will strengthen the validity and clinical applicability of our observations.

Conclusion

This study provides a comprehensive characterization of nasal microbiome-host interactions in CRSwNP and NIP, revealing both disease-specific and shared gene-microbe associations linked to distinct clinical features. By illuminating these mucosal-microbial networks, our work establishes a foundational framework for investigating mechanisms of nasal dysbiosis and identifies potential therapeutic targets for precision intervention. The findings advance understanding of nasal disease pathophysiology while offering translational opportunities for microbiome-modulating strategies in rhinological disorders.

Ethical approval and consent to participate

This study was approved by the Ethics Research Committees of the Tianjin First Central Hospital (Approval number. 2021N037KY). This study was performed in accordance with the relevant guidelines and regulations. Written informed consent was obtained from all participants.

Consent for publication

Not applicable.

Availability of data and materials

We declare that the main data supporting the finding of this study are available within the paper and its Supplementary Materials. The clean reads were deposited in the National Center for Biotechnology Information (NCBI) Sequence Read Archive (SRA) database (Accession no. PRJNA997619). The raw transcriptomic data for the human cohort have been deposited in the NCBI under GSE255573 for controlled access.

Competing interests

The authors declare that they have no competing interests.

Funding

This work was supported by Tianjin Health Research Project (Grant Nos. TJWJ2022XK020); National Natural Science Foundation of China (Grant Nos. 82401333); and Tianjin Natural Science Foundation (Grant Nos. 24JCQNJC01170).

Authors' contributions

YL, ZC, JZ, and GZ all developed the study concept and design. CZ, ZL and JL collected nasal samples. CZ, WS and JL guided sta-

tistical analysis and data analysis. YL, ZC, JZ, and GZ verified the experimental design, visualized the experimental results, and critically reviewed the manuscript. YL, CZ, ZL and JL recruited patients and collected specimens, collected clinical metadata, interpreted the microbiome data, and were major contributors in writing the manuscript and reviewing it critically. The authors read and approved the final manuscript.

Acknowledgement

The authors thank all the subjects who participated in this study. This work was funded by Tianjin Key Medical Discipline Construction Project.

References

1. Fokkens WJ, Viskens AS, Backer V, et al. EPOS/EUFOREA update on indication and evaluation of biologics in Chronic Rhinosinusitis with Nasal Polyps 2023. Rhinology. 2023 Jun 1;61(3):194-202.
2. Yu S, Grose E, Lee DJ, Wu V, Pellarin M, Lee JM. Evaluation of inverted papilloma recurrence rates and factors associated recurrence after endoscopic surgical resection: a retrospective review. J Otolaryngol Head Neck Surg. 2023 Apr 27;52(1):34.
3. Du K, Zhao Y, Zhang X, et al. Staphylococcus aureus lysate induces an IgE response via memory B cells in nasal polyps. J Allergy Clin Immunol. 2024 Mar;153(3):718-731.e11.
4. Rha MS, Kim CH, Yoon JH, Cho HJ. Association of the human papillomavirus infection with the recurrence of sinonasal inverted papilloma: a systematic review and meta-analysis. Rhinology. 2022 Feb 1;60(1):2-10.
5. Priya S, Burns MB, Ward T, et al. Identification of shared and disease-specific host gene-microbiome associations across human diseases using multi-omic integration. Nat Microbiol. 2022 Jun;7(6):780-795.
6. Lloyd-Price J, Arze C, Ananthakrishnan AN, et al. Multi-omics of the gut microbial ecosystem in inflammatory bowel diseases. Nature. 2019 May;569(7758):655-662.
7. Flemer B, Lynch DB, Brown JM, et al. Tumour-associated and non-tumour-associated microbiota in colorectal cancer. Gut. 2017 Apr;66(4):633-643.
8. Fokkens WJ, Lund VJ, Hopkins C, et al. European Position Paper on Rhinosinusitis and Nasal Polyps 2020. Rhinology. 2020 Feb 20;58(Suppl S29):1-464.
9. Fuks G, Elgart M, Amir A, et al. Combining 16S rRNA gene variable regions enables high-resolution microbial community profiling. Microbiome. 2018 Jan 26;6(1):17.
10. Hu S, Bourgonje AR, Gacesa R, et al. Mucosal host-microbe interactions associate with clinical phenotypes in inflammatory bowel disease. Nat Commun. 2024 Feb 17;15(1):1470.
11. Nejman D, Livyatan I, Fuks G, et al. The human tumor microbiome is composed of tumor type-specific intracellular bacteria. Science. 2020 May 29;368(6494):973-980.
12. Sato N, Tamada Y, Yu G, Okuno Y. CBNplot: Bayesian network plots for enrichment analysis. Bioinformatics. 2022 May 13;38(10):2959-2960.
13. Yu J, Chen Y, Fu X, et al. Invasive Fusobacterium nucleatum may play a role in the carcinogenesis of proximal colon cancer through the serrated neoplasia pathway. Int J Cancer. 2016 Sep 15;139(6):1318-26.
14. Kato A, Schleimer RP, Bleier BS. Mechanisms and pathogenesis of chronic rhinosinusitis. J Allergy Clin Immunol. 2022 May;149(5):1491-1503.
15. Kim SJ, Park JH, Lee SA, Lee JG, Shin JM, Lee HM. All-trans retinoic acid regulates TGF-β1-induced extracellular matrix production via p38, JNK, and NF-κB-signaling pathways in nasal polyp-derived fibroblasts. Int Forum Allergy Rhinol. 2020 May;10(5):636-645.
16. Huang ZQ, Zhou XM, Yuan T, et al. Epithelial tight junction anomalies in nasal inverted papilloma. Laryngoscope. 2024 Feb;134(2):552-561.
17. Xu Z, Huang Y, Meese T, et al. The multiomics single-cell landscape of sinus mucosa in uncontrolled severe chronic rhinosinusitis with nasal polyps. Clin Immunol. 2023 Nov;256:109791.
18. Liao S, Huang Y, Zhang J, et al. Vitamin D promotes epithelial tissue repair and host defense responses against influenza H1N1 virus and Staphylococcus aureus infections. Respir Res. 2023 Jul 5;24(1):175.
19. Glaviano A, Foo ASC, Lam HY, et al. PI3K/AKT/mTOR signaling transduction pathway and targeted therapies in cancer. Mol Cancer. 2023 Aug 18;22(1):138.
20. Liang Y, Mao J, Qiu T, et al. Predicting nasal diseases based on microbiota relationship network. Sci Prog. 2025 Jan-Mar;108(1):368504251320832.
21. Lin L, Yi X, Liu H, et al. The airway microbiome mediates the interaction between environmental exposure and respiratory health in humans. Nat Med. 2023 Jul;29(7):1750-1759.
22. Liang Y, Xie R, Xiong X, et al. Alterations of nasal microbiome in eosinophilic chronic rhinosinusitis. J Allergy Clin Immunol. 2023 May;151(5):1286-1295.e2.
23. Kidoguchi M, Imoto Y, Noguchi E, et al. Middle meatus microbiome in patients with eosinophilic chronic rhinosinusitis in a Japanese population. J Allergy Clin Immunol. 2023 Dec;152(6):1669-1676.e3.
24. Hu S, Bourgonje AR, Gacesa R, et al. Mucosal hostmicrobe interactions associate with clinical phenotypes in inflammatory bowel disease. Nat Commun. 2024 Feb 17;15(1):1470.
25. Fu K, Cheung AHK, Wong CC, et al. Streptococcus anginosus promotes gastric inflammation, atrophy, and tumorigenesis in mice. Cell. 2024 Feb 15;187(4):882-896.e17.
26. Li Y, Tong T, Li P, et al. Screening of potential probiotic Lactobacillaceae and their improvement of type 2 diabetes mellitus by promoting PI3K/AKT signaling pathway in db/db mice. Pol J Microbiol. 2023 Sep 20;72(3):285-297.
27. Li Z, Lu G, Li Z, et al. Altered actinobacteria and firmicutes phylum associated epitopes in patients with Parkinson's disease. Front Immunol. 2021 Jul 2;12:632482.
28. Luo C, Peng S, Li M, Ao X, Liu Z. The efficacy and safety of probiotics for allergic rhinitis: a systematic review and meta-analysis. Front Immunol. 2022 May 19;13:848279.
29. Iwasaki N, Poposki JA, Oka A, et al. Single cell RNA sequencing of human eosinophils from nasal polyps reveals eosinophil heterogeneity in chronic rhinosinusitis tissue. J Allergy Clin Immunol. 2024 Oct;154(4):952-964

*Jingtai Zhi
E-mail: 15900294033@163.com
* Guimin Zhang
E-mail: zh_gm@163.com

Department of Otorhinolaryngology
Head and Neck Surgery
Tianjin First Central Hospital
Institute of Otolaryngology of Tianjin
Key Laboratory of Auditory Speech and Balance Medicine
Key Clinical Discipline of Tianjin (Otolaryngology)
Otolaryngology Clinical Quality Control Centre
300192 Tianjin
China

Yibo Liang[1,#], Zheming Chen[2,#], Chenting Zhang[1,3,#], Zhili Li[1], Jiarui Liu[1], Wenjuan Sun[2], Jianxin Li[2], Jingtai Zhi[1,*], Guimin Zhang[1,*]

[1] Department of Otorhinolaryngology Head and Neck Surgery, Tianjin First Central Hospital, Institute of Otolaryngology of Tianjin, Key Laboratory of Auditory Speech and Balance Medicine, Key Medical Discipline of Tianjin (Otolaryngology), Quality Control Centre of Otolaryngology, Tianjin, China

[2] LC-BIO Technologies CO., LTD., Hangzhou, China

[3] Department of Head and Neck Tumor Surgery, Shanxi Provincial People's Hospital, Shanxi, China

[#] contributed equally

Rhinology 63: 6, 753 - 764, 2025
https://doi.org/10.4193/Rhin24.386

Received for publication:
September 5, 2024
Accepted: June 17, 2025

Associate Editor:
Michael Soyka

This manuscript contains online supplementary material

SUPPLEMENTARY MATERIAL

Materials and methods

Subject recruitment and sampling

Each patient underwent a physical examination by two rhinologists to confirm the diagnosis, and clinical information such as age, sex, smoking history, medication history, and surgical history was recorded.

5R 16S rRNA gene sequencing and analyses

To better characterize the microbiota in nasal tissues, 5R 16S sequencing was used in this study. In brief, nasal tissue and negative controls were extracted via the Cetyl Trimethyl Ammonium Bromide method. All negative controls included sampling controls, DNA extraction controls and no-template PCR amplification controls. The modified 5R 16S rRNA gene was amplified. The modified 5R 16S rRNA gene is composed of five regions (the V2, V3, V5, V6, and V8 regions). The amplified products were then purified and quantified by standardized means. The purified products were then sequenced on the Illumina NovaSeq platform supported by Lc-Bio Technologies Co., Ltd. (Hangzhou, China). After the sample sequencing data were removed, the high-quality sequences that remained after the removal of low-quality sequencing results were used for subsequent analysis.

The reads were demultiplexed per sample, filtered and aligned to each of the five amplified regions based on the primer sequences. The SMURF (short multiple regions framework) method was applied to combine read counts from the five regions into coherent profiling results to solve the maximum likelihood problem [13]. Then, the taxonomic identification and relative abundance calculation of bacteria were carried out. The database that was used in this project is optimized Greengenes (May 2013 version).

Subsequent microbiome diversity analysis and microbiome difference analysis were carried out on the basis of these data. The richness and uniformity of alpha diversity are mainly reflected by indices such as Chao1 and observed species. Beta diversity analysis usually begins by calculating the distance matrix between environmental samples, which includes the distance between any two samples. Beta diversity, together with alpha diversity, constitutes the overall diversity or the biological heterogeneity of a given environmental community. The Kruskal-Wallis test was used to compare multiple groups with biological duplicate samples.

Bioinformatics analysis of RNA-seq data

As previously mentioned, the RNA was isolated and purified from the total sample using a standardized process. Then, the quantity and purity of the isolated RNA were controlled, and the integrity of the RNA was tested. After two rounds of purification, mRNA with poly(A) (polyadenylate) was specifically captured. The captured mRNA was fragmented at high temperature with the NEBNextR RNA Fragmentation Module (NEB, cat. e6150, USA) at 94°C for 5-7 minutes. cDNA was synthesized from the fragmented RNA with Invitrogen SuperScriptTM II Reverse Transcriptase (Invitrogen, cat. 1896649, USA). E. coli DNA polymerase I (NEB, cat.m0209, USA) and RNase H (NEB, cat.m0297, USA) were then used for two-strand synthesis. To preserve the orientation information of the transcript during transcriptome sequencing, these complex double strands of DNA and RNA were converted into double-stranded DNA, and dUTP Solution (Thermo Fisher, cat. R0133, CA, USA) was added to the double strands to convert the ends of the double-stranded DNA into flat ends. Then, an A base is added to each end so that it could be connected to the terminal with T base joints, and the size of the fragment was screened and purified by magnetic beads. The double-stranded library was digested with UDG enzyme (NEB, cat. m0280, MA, US) and then formed by PCR with a fragment size of 300 bp±50 bp (chain-specific library). Finally, we used an Illumina NovaSeqTM 6000 (LC Bio Technology Co., Ltd.; Hangzhou, China) to perform double-end sequencing in PE150 mode according to standard procedures. The sequence information of the transcripts that were obtained by sequencing was only derived from the first strand.

After using Cutadapt to remove unqualified sequences (sequencing joints, low-quality sequences, etc.) from the original data to obtain valid data (clean data), reference genome alignment was performed using HISAT2. Based on the HISAT2 comparison results, Stringtie was used to reconstruct the transcripts and calculate the expression levels of all the genes in each sample. Gene expression level analysis mainly aimed to analyze protein-coding genes (mRNAs) that were annotated by the genome, and the expression levels of genes were statistically measured to evaluate the correlation of gene expression characteristics and differentially expressed genes within and between groups. When measuring gene expression levels, fragments per kilobase million (FPKM) values, which are standardized based on the original read counts of genes, were used as measures of gene expression levels, and gene expression levels in different samples were quantified. The results of differential expression gene analysis, differential expression gene enrichment analysis and GSVA were obtained in the set comparison group.

Sparse CCA analysis

We used a machine learning framework that was developed by Priya et al. [6] to integrate high-dimensional datasets of host

gene expression and microbiome abundance. SparseCCA was used to determine group-level correlations between paired host gene expression and microbiome data in each disease cohort. sparseCCA performs feature selection via the L1 or lasso penalty while maximizing the correlation between the two datasets. Its objective function can be expressed as:

$$maximize_{u,v} u^T X^T Y v \; subject\; to\; u^T X^T X u \leq 1, v^T Y^T Y v \leq 1, \|u\|_1 \leq \lambda_1, \; , \|v\|_1 \leq \lambda_2,$$

where X and Y represent two data matrices with the same number of samples but different numbers of features (representing microbiome taxa composition data and host gene expression data, respectively). u and v are the canonical load vectors of X and Y, respectively; λ1 and λ2 control the lasso penalty of U and V, respectively. τ represents the transpose of a matrix. As with the original method, leave-one-out cross-validation was used for a grid-search approach to obtain the optimal hyperparameters. Using this method, λ1 and λ2 for group CRSwNP were set to 0.2 and 0.15, respectively, and λ1 and λ2 for group NIP were set to 0.266 and 0.177, respectively. After the sparsity parameters were determined, the sparse CCA model was fitted to obtain a subset of the relevant host genes and microorganisms (called components), calculating only the top 10 components for each disease cohort. Additionally, the leave-one-out cross-validation approach was used to calculate the importance of each component. Cor.test was used to evaluate the true strength and significance of the association, and Benjamini-Hochberg (FDR) was used to correct the P value of the multiple hypothesis test for each disease cohort. Only significant components with FDR < 0.1 were retained. Based on this method, three important components in group CRSwNP were identified, with an average of 1739 host genes and 4.5 microorganisms. There were six significant components in group NIP, with an average of 2,786 host genes and 6.4 microbes. sparseCCA was applied separately for each disease cohort using the R language (version 4.2.0) package "PMA" (version 1.2.1). All the components were visualized using Cytoscape (version 3.10.0).

Fluorescence in situ hybridization (FISH)

FISH is performed using probes that target the 16S rRNA gene sequence for a specific bacterial taxon. According to previous methods, the *Geobacillus* FISH probe was hybridized to tissue sections and labeled with FITC at the 5' and 3' ends (5'CCGAATCAAGGCAAGCCCCAATC-3'). This probe was designed and synthesized by Exonbio (Gungzhou, China). This probe targets *Geobacillus stearothermophilus*, and some *Geobacillus* sp. EUB330 proteins target a conserved domain of bacterial 16S rRNA. FISH images were captured with a Nikon 80i microscope. The images were analyzed and scored according to the fluorescence signal.

Western blotting

Tissues were homogenized in liquid nitrogen, and an appropriate amount of RIPA cell lysis was added. After centrifugation, the concentration of superalbumin was extracted and determined. The protein concentration was determined by the BCA method. The proteins were denatured by boiling after the original volume of buffer was added. After protein electrophoresis and membrane transfer, the membranes were blocked in BSA solution at room temperature, and the membranes were incubated with primary antibodies (rabbit anti-p65, ab32536; rabbit anti-p-p65, ab109458; rabbit anti-β-actin, ab8227) at 4°C overnight. The next day, after the membrane was washed with the washing liquid and incubated at room temperature with the secondary antibody for 1 hour. After the membrane was washed with the washing liquid, ECL was applied for color development. The original gels are shown in Figure S1.

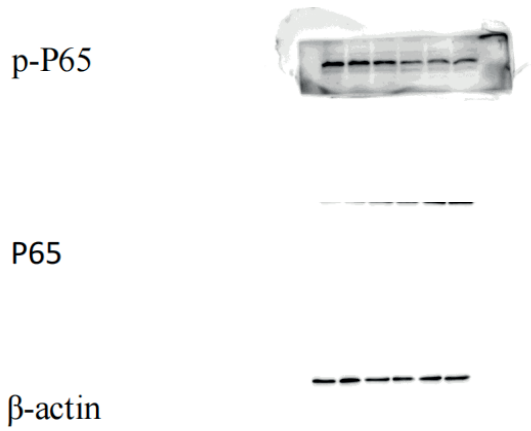

Figure S1. The original gels of p65 and p-p65 are shown.

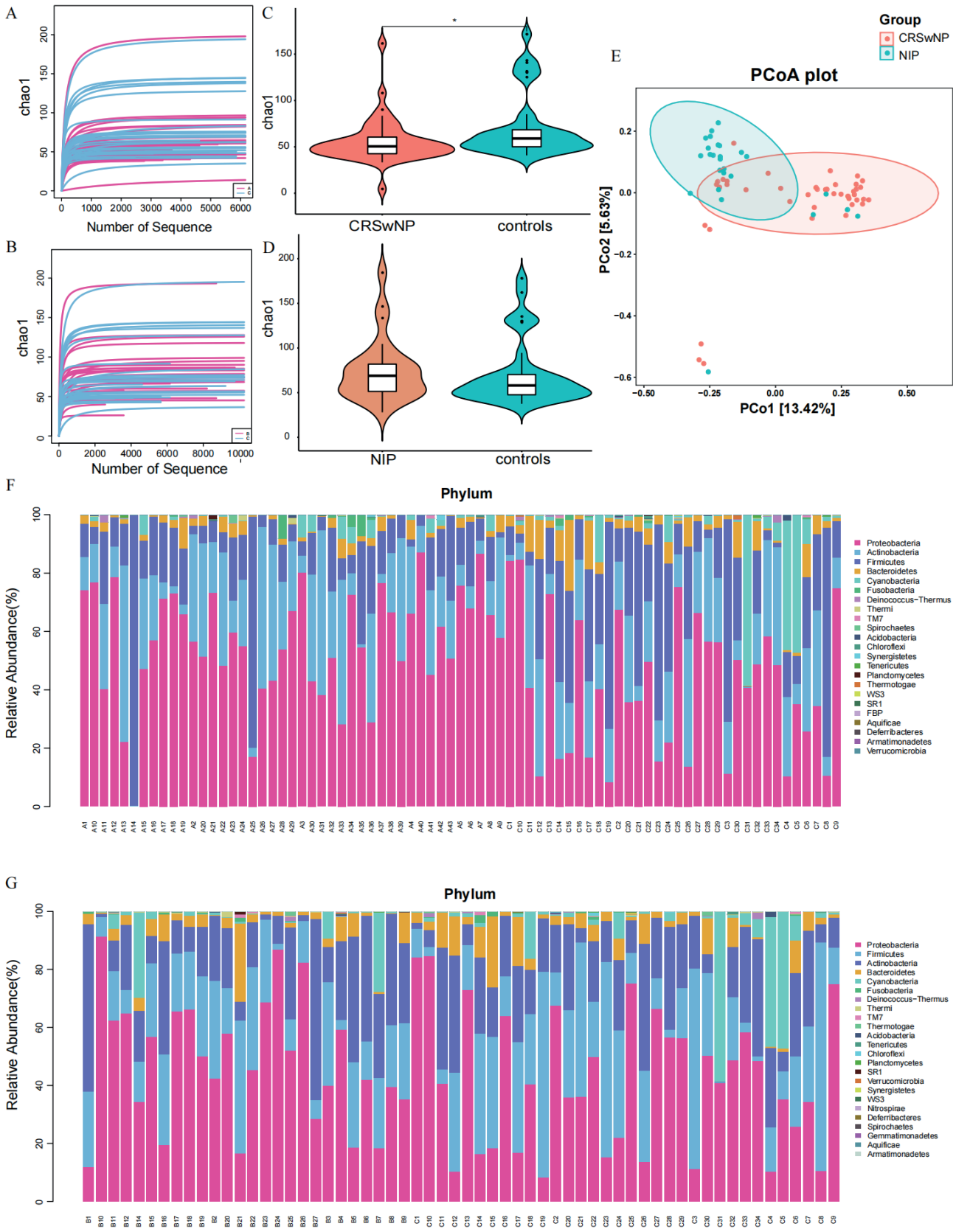

Figure S2. Dilution curve in observed OTUs of CRSwNP (A)/ NIP(B) and controls. (C) The Chao1 index were significantly decreased in CRSwNP patients compared with controls. (D) Compared with the controls, the Chao1 index of NIP patients was increased but not significantly. (E) PCoA indicates a partial but significant separation between patients with CRSwNP and NIP. (F) Relative proportions of bacterial phyla in CRSwNP patients and controls. (G) Relative proportions of bacterial phyla in NIP patients and controls.

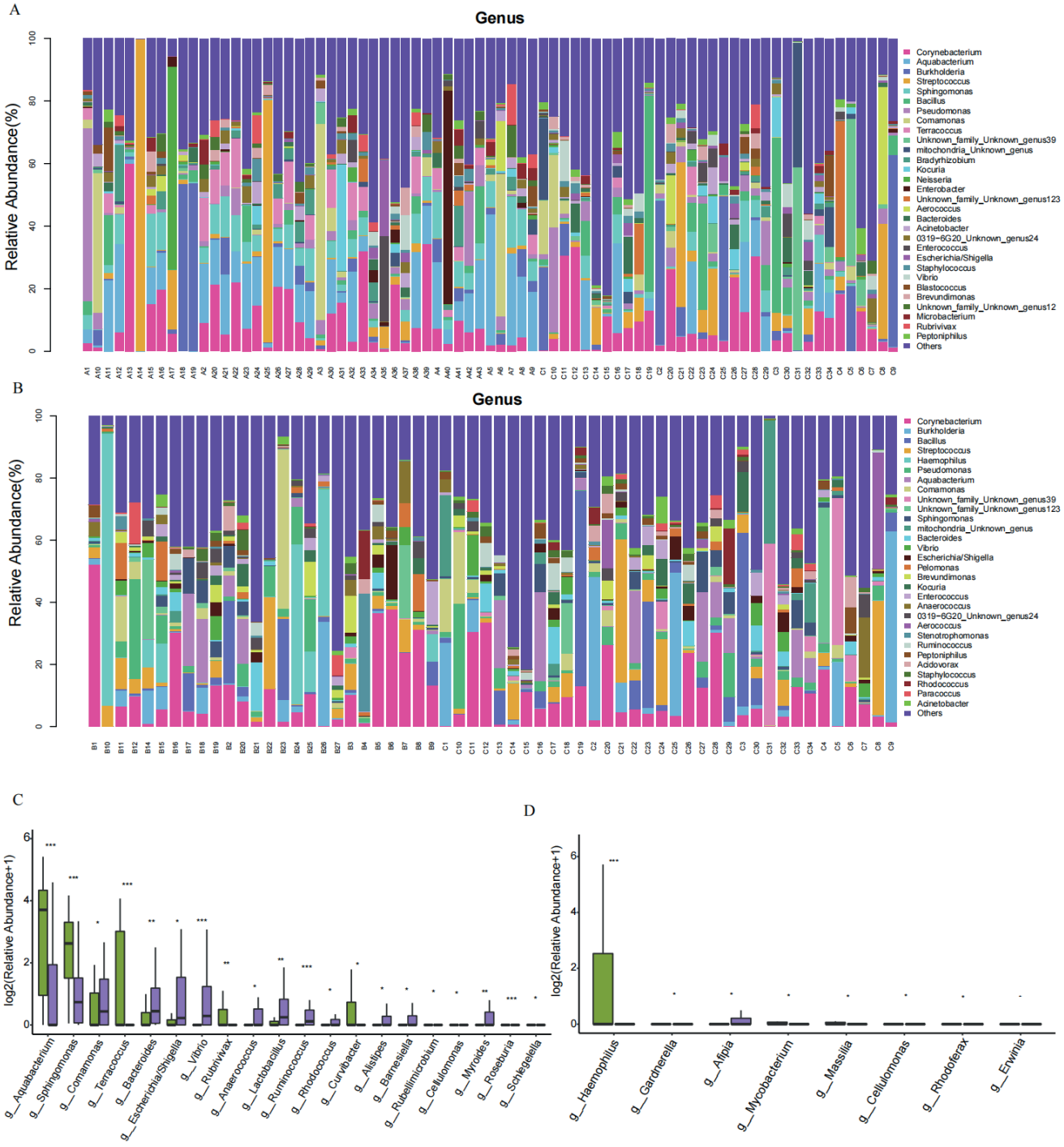

Figure S3. (A) Relative proportions of bacterial genus in CRSwNP patients and controls. (B) Relative proportions of bacterial genus in NIP patients and controls. (C) Statistically differential genus of nasal microbiota were evaluated with box plots between CRSwNP and controls. (D) Statistically differential genus of nasal microbiota were evaluated with box plots between NIP and controls.

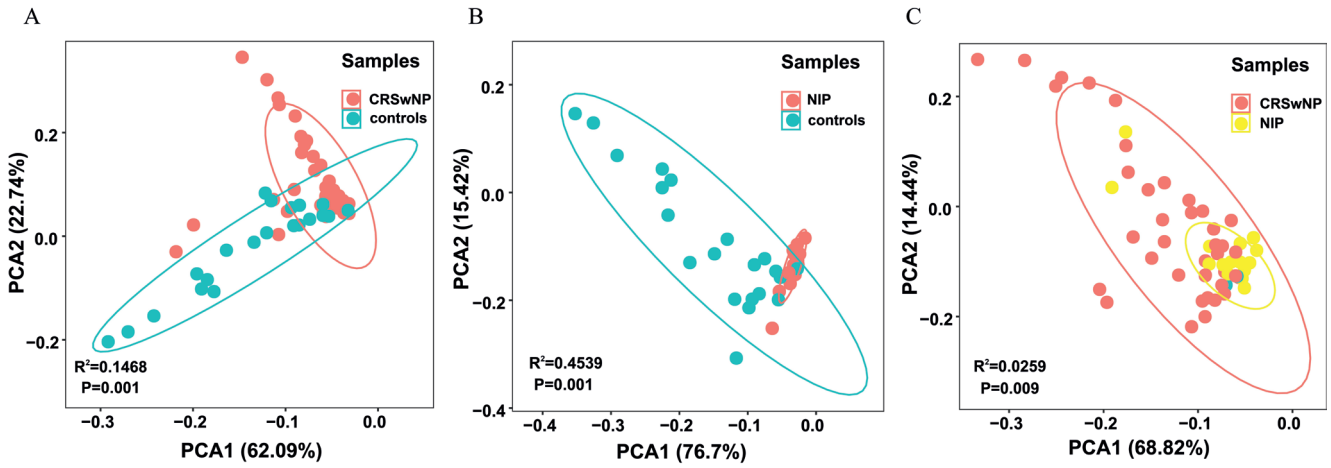

Figure S4. (A) Principal component analysis indicates significant separation among CRSwNP and controls for host transcriptome. (B) Principal component analysis indicates significant separation among NIP and controls for host transcriptome. (C) Principal component analysis indicates significant separation among CRSwNP and NIP for host transcriptome.

Table S1. Demographic characteristics of the cohorts.

Pathology	CRSwNP (n=43)	NIP (n=27)	Controls (n=34)	χ^2 or F	P
Age (years)	47.86 ± 11.985	55.26 ± 13.265	41.76 ± 12.589	8.739	<0.001
gender					
Male, n (%)	26 (60.5%)	17 (63.0%)	27 (79.4%)	3.410	0.182
Female, n (%)	17 (39.5%)	10 (37.0%)	7 (20.6%)		
Atopy, n (%)					
0	22 (51.2%)	23 (85.1%)	22 (64.7%)	8.378	0.015
1	21 (48.8%)	4 (14.8%)	12 (35.3%)		
Never smoker, n (%)					
0	26 (60.5%)	16 (59.3%)	22 (64.7%)	0.224	0.894
1	17 (39.5%)	11 (40.7%)	12 (35.3%)		
Serum total IgE (kU/l)	47.40 (18.60,198.00)	27.30 (7.68,111.00)	21.65 (9.03,113.00)	5.086	0.079
Lund–Mackay CT score	15.00 (11.00,19.00)	5.00 (4.00,8.00)	0.00 (0.00,0.00)	87.197	<0.001